Clays and Clay Minerals, Vol. 52, No. 3, 321–333, 2004.

COPPER SORPTION MECHANISMS ON SMECTITES

DANIEL G. STRAWN[1,*], NOEL E. PALMER[1], LUCA J. FURNARE[1], CARMEN GOODELL[1], JAMES E. AMONETTE[2] AND RAVI K. KUKKADAPU[2]

[1] Department of Plant, Soil and Entomological Sciences, University of Idaho, Moscow, ID 83844-2339, USA
[2] Pacific Northwest National Laboratory, Richland, Washington, USA

Abstract—Due to the importance of clay minerals in metal sorption, many studies have attempted to derive mechanistic models that describe adsorption processes. These models often include several different types of adsorption sites, including permanent charge sites and silanol and aluminol functional groups on the edges of clay minerals. To provide a basis for development of adsorption models it is critical that molecular-level studies be done to characterize sorption processes. In this study we conducted X-ray absorption fine structure (XAFS) and electron paramagnetic resonance (EPR) spectroscopic experiments on copper (II) sorbed on smectite clays using suspension pH and ionic strength as variables. At low ionic strength, results suggest that Cu is sorbing in the interlayers and maintains its hydration sphere. At high ionic strength, Cu atoms are excluded from the interlayer and sorb primarily on the silanol and aluminol functional groups of the montmorillonite or beidellite structures. Interpretation of the XAFS and EPR spectroscopy results provides evidence that multinuclear complexes are forming. Fitting of extended X-ray absorption fine structure spectra revealed that the Cu-Cu atoms in the multinuclear complexes are 2.65 Å apart, and have coordination numbers near one. This structural information suggests that small Cu dimers are sorbing on the surface. These complexes are consistent with observed sorption on mica and amorphous silicon dioxide, yet are inconsistent with previous spectroscopic results for Cu sorption on montmorillonite. The results reported in this paper provide mechanistic data that will be valuable for modeling surface interactions of Cu with clay minerals, and predicting the geochemical cycling of Cu in the environment.

Key Words—Copper, EPR, EXAFS, Montmorillonite, Smectite, Sorption.

INTRODUCTION

An important characteristic of clay minerals is their large cation adsorption capacity. The classic model of cation adsorption on clay minerals implies that adsorption occurs in the interlayers via electrostatic interactions (outer-sphere adsorption complexes) (Marshal, 1935; Sposito, 1989). Recent research suggests that inner-sphere adsorption on ligand functional groups located at mineral discontinuities (edges, steps and kinks) of clay minerals is also important (Bradbury and Baeyens, 1999; Dahn *et al.*, 2003; Morton *et al.*, 2001; Papelis and Hayes, 1996; Schlegel *et al.*, 1999; Zachara *et al.*, 1993). Evidence for the existence of inner-sphere complexation has been provided by theoretical modeling of metal sorption behavior (Helmy *et al.*, 1994; Schindler *et al.*, 1987; Stadler and Schindler, 1993; Undabeytia *et al.*, 2002; Zachara and McKinley, 1993). However, this approach often suffers from lack of molecular-level evidence of the sorption processes. Schlegel *et al.* (1999) and Dahn *et al.* (2003) used polarized EXAFS spectroscopy to provide direct evidence for the formation of inner-sphere linkages of Co and Ni, respectively, on clay minerals without the formation of multinuclear complexes.

Many researchers investigating edge-site sorption on clay minerals have instead observed multinuclear complexes (Hyun *et al.*, 2000; Morton *et al.*, 2001; O'Day *et al.*, 1994; Strawn and Sparks, 1999). The existence of multinuclear metal complexes on clay minerals has been shown for several metals, including Pb, Co, Cu, Cd, Ni and Zn (Di Leo and O'Brien, 1999; Morton *et al.*, 2001; O'Day *et al.*, 1994; Papelis and Hayes, 1996; Schlegel *et al.*, 2001). Of particular interest is that these complexes are forming in systems in which they are not predicted to be present in aqueous solution based on known thermodynamic equilibrium constants. The occurrence of multinuclear complexes in clay suspensions undersaturated with respect to the metal hydrolysis complexes suggests that clay minerals are enhancing their formation. Three common hypotheses are often presented to explain enhanced surface precipitation: (1) due to the surface charge, the properties of the water molecules next to the surface are altered (dielectric saturation); this has direct impacts on metal hydrolysis equilibrium; (2) stearic or nucleation enhancement occurs due to multi-layer sorption on specific sorption sites; and (3) mixed-cation multinuclear complexes form using cations in solution and cations dissolved from the mineral (solid-solution) (O'Day *et al.*, 1994; Strawn and Sparks, 1999; Towle *et al.*, 1997). While multinuclear complex formation on clay minerals has been suggested for many years (McBride, 1982b), recent advances in molecular spectroscopy have made it

* E-mail address of corresponding author:
dgstrawn@uidaho.edu
DOI: 10.1346/CCMN.2004.0520307

Copyright © 2004, The Clay Minerals Society

https://doi.org/10.1346/CCMN.2004.0520307 Published online by Cambridge University Press

possible to make direct observations into the molecular structure and location of these complexes.

The present research is focused on the transition metal copper. Several papers have reported the occurrence of multinuclear Cu complexes on minerals (Cheah *et al.*, 2000; Farquhar *et al.*, 1996; McBride, 1982a; McBride and Bouldin, 1984; Morton *et al.*, 2001; Weesner and Bleam, 1997). McBride (1982b) assigned the loss of EPR signal intensity in hectorite suspensions undersaturated with respect to $Cu(OH)_2$ (s) to the formation of aqueous multinuclear complexes such as $Cu_2(OH)_2^{2+}$ in the clay interlayer. Ford and Sparks (1998) reported that Cu sorbed onto pyrophyllite lacked a second neighbor atom, while Zn sorbed under similar equilibration conditions formed a vast multinuclear mixed-cation precipitate.

Morton *et al.* (2001) used extended X-ray absorption fine structure (EXAFS) spectroscopy to determine how equilibrium conditions (ionic strength (*I*) and pH) impact Cu complexation mechanisms on montmorillonite. At low ionic strength and pH, sorbed Cu was observed to maintain its hydration sphere, while at higher ionic strengths and pH, sorbed Cu had second-shell Cu atoms located 2.98 Å apart, indicating that the sorbed Cu existed in a multinuclear complex with structural similarities to $Cu(OH)_2$ (s) (Morton *et al.*, 2001). Farquhar *et al.* (1996) investigated Cu complexation on the (001) mica surface using EXAFS spectroscopy and X-ray photoelectron spectroscopy (XPS) and observed the formation of multinuclear complexes having Cu–Cu distances of 2.65 Å. Cu–Cu bond distances of 2.65 Å have been reported for Cu in the Cu-silicate mineral plancheite and for Cu sorbed on amorphous silica (Cheah *et al.*, 1998; Farquhar *et al.*, 1996). Cheah *et al.* (1998) noted that at low loading levels Cu formed small Cu dimers on the surface of SiO_2, and as the surface loading increased, multinuclear complexes consistent with $Cu(OH)_2$ (s) formed (Cheah *et al.*, 2000).

In this study we are investigating Cu sorption on montmorillonite and beidellite as a function of varying ionic strength and pH. In contrast to the study of Morton *et al.* (2001), we have selected initial equilibrium conditions that are undersaturated with respect to CuO (s), thus resulting in lower loading levels, and used Ca^{2+} as the competing ion to isolate more effectively the permanent charge sites in the interlayers. Results from this study will support the development of a mechanistic understanding for the enhanced formation of multinuclear metal complexation by clay minerals.

METHODS

Clay minerals

SWy-2 montmorillonite and SBId-1 beidellite were purchased from the Source Clays Repository (Purdue University, Indiana). Beidellite is a dioctahedral clay mineral with isomorphic substitution occurring predominantly in the tetrahedral sheet, as opposed to montmorillonite that has isomorphic substitution in the octahedral sheet. Preparation of the clay minerals entailed grinding in a ball mill to reduce particle size, successive treatment with Na hypochlorite at 50ºC to remove trace amounts of organic matter, washing at 50ºC with acetate buffer solution to dissolve carbonates, saturation with Na ions, complete dialysis to remove non-sorbed ions and chemicals, particle-size separation via centrifugation to isolate the 0.2–2 μm size fraction, and freeze drying to dry the clays into powders. X-ray diffraction and diffuse reflectance-Fourier transform infrared (DRIFT) measurements were made on the treated clay to ensure purity. To test for the influence of free Fe oxyhydroxides, selected samples were treated with citrate-bicarbonate-dithionite solution (CBD) to remove any Fe minerals. The XAFS spectroscopy results (data not shown) for the CBD-treated clays were identical to non-CBD-treated samples.

pH edges

All experiments were conducted using deionized water that was boiled and cooled by degassing with N_2 (g). Copper solutions were made from nitrate salts. Sorption-pH edges were conducted at two ionic strengths, 0.001 M and 0.1 M calcium nitrate. Experiments comparing Ca, Mg, K and Na showed that Ca is much more effective at excluding Cu from the interlayers than the other cations.

At the onset of the experiments, the clay minerals were preequilibrated in the background electrolytes at pH = 4 for 24 h. The solid-solution ratio was 10 g L^{-1}. Following preequilibration, the clays were spiked with a Cu stock solution to achieve a final Cu concentration of 3.6×10^{-5} M. After the clay suspensions were spiked, the samples were allowed to mix for 10 min. Next, a 10 mL aliquot was removed and placed in a centrifuge tube. The pH of the bulk suspension was increased by 0.5 pH unit increments, and 10 mL subsamples were removed at each increment and placed in centrifuge tubes for equilibration. The samples were incubated for 24 h on an end-over-end shaker at 23–26ºC. Following equilibration, the samples were centrifuged and filtered through a membrane filter (0.2 μm). Solutions were acidified by adding 1 drop (~0.1 mL) of concentrated nitric acid. Aqueous metal concentrations were determined by inductively coupled plasma atomic emission spectroscopy (ICP-AES) using NIST traceable standards. The amount of metal sorbed was calculated from the difference between the initial and final aqueous metal concentrations. Initial concentration was taken from a blank (no clay) run through the experiment at pH $\approx$3.

XAFS sample preparation

To prepare samples for XAFS analysis, 30 mL of clay suspensions (1:50 solid:solution gravimetric) were placed in dialysis bags (Spectrapor 3500 dalton) and

https://doi.org/10.1346/CCMN.2004.0520307 Published online by Cambridge University Press

suspended in 970 mL of 4.0×10^{-5} M Cu solution with I and pH preadjusted. After 8–12 h of incubation, the Cu solution was replaced with fresh Cu solution, pH preadjusted. The pH was monitored and adjusted throughout the equilibration. The high solid to solution ratio (effectively 1/1000), and replenishment of Cu solution allowed us to load the clays with high concentrations of Cu without having high aqueous Cu concentrations, thereby avoiding oversaturation with respect to Cu (hydr)oxides. The Cu concentration was selected so that the initial [Cu] in all samples was below the concentration at which Cu precipitation or hydrolysis is expected. Copper hydrolysis and precipitation speciation were evaluated using constants in the *Mineql* database (Schecher, 1998) and from Baes and Mesmer (1986). At the equilibration conditions used in our experiments, CuO (s) is the least soluble Cu mineral. A CuO (s) solubility diagram is shown in Figure 1, along with sample equilibration conditions used in these experiments.

XAFS experiments

The XAFS data acquisition of the Cu K-edge (8979 eV) was conducted on beamline 4 at stations 4.1, 4.2 and 4.3 at the Stanford Synchrotron Radiation Laboratory (SSRL). The electron beam energy was 3 GeV, and the beam current ranged from 100 to 60 mA. The monochromator consisted of two parallel Si(111) crystals with an entrance slit of 2 mm. Harmonic rejection was achieved by detuning the second crystal 40%. For X-ray absorption near edge structure (XANES) data collection, the mono-entrance slit was decreased to 1 mm and detuning was reduced to 30% to increase resolution and signal counts, respectively. The XAFS data were collected in fluorescence mode using a 13-element Ge detector. The spectra of Cu standards were collected in fluorescence mode using an argon purged Stern-Heald type detector (Lytle *et al.*, 1984), as well as transmission using N_2-filled ionization chambers. Clay-mineral samples were loaded in a plastic sample cell, sealed with Kapton® tape, and stored in airtight plastic bags until analysis. Standards were diluted in boron nitride to achieve the desired absorbance. A Cu foil was used in all experiments as an internal standard to calibrate the beam energy. The spectra were collected at room temperature (~298 K).

The XAFS data analysis was accomplished using the program *WinXAS* (Ressler, 1998) and *FEFF*8.0 (Ankudinov *et al.*, 1998). The spectra were processed using the following procedure: (1) multiple scans were merged and energy calibrated to the Cu K-edge (8979 eV); (2) the spectra were normalized to unit-step height using a linear pre- and post-edge background subtraction; (3) the spectra were transformed to k-space using the inflection point of the sample-edge jump; (4) the χ-function was extracted from the raw data by

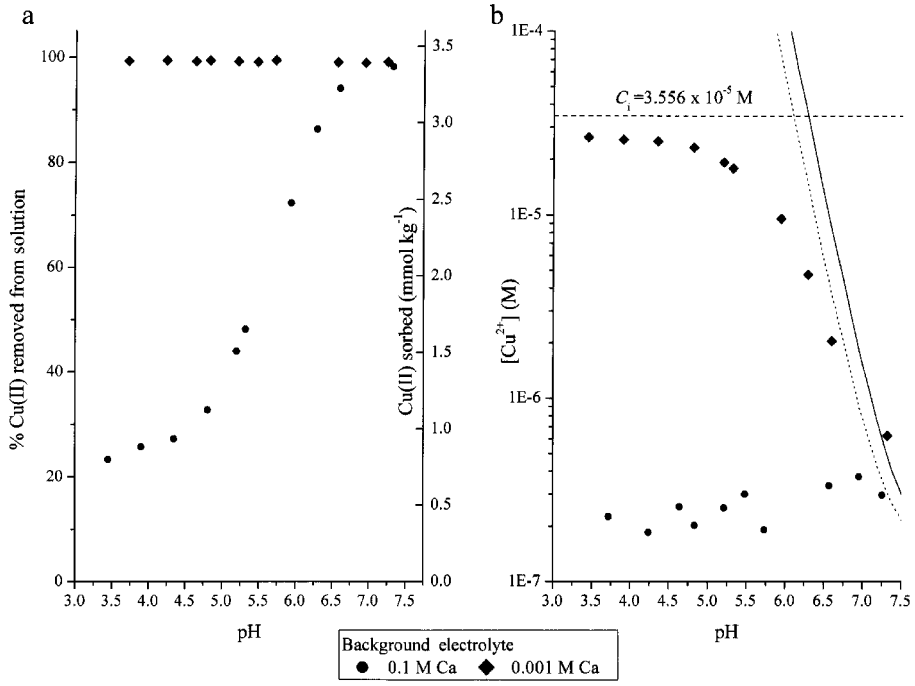


Figure 1. Sorption behavior of Cu on montmorillonite as a function of pH and ionic strength (I). Montmorillonite concentration was 10 g L^{-1}, initial Cu concentration (C_i) was 3.6×10^{-5} M. Figure 1a show the percentage of Cu left in solution and the sorbed Cu concentration (right axis). Figure 1b shows the equilibrium [Cu] in the Ca background electrolyte experiment as a function of pH, as well as the solubility line for tenorite (CuO) at two ionic strengths. The solid line in 1b is CuO solubility at $I = 0.001$ and dotted line is CuO solubility at $I = 0.1$.

https://doi.org/10.1346/CCMN.2004.0520307 Published online by Cambridge University Press

subtracting the atomic background using a cubic-spline consisting of 5 knots set at equal distances fit to k^3-weighted data; and (5) the data were Fourier transformed (FT) to isolate individual frequencies in the $\chi(k^3)$ spectra (k range for FT was ~3.4–11.8 $Å^{-1}$). For background removal (step 4), the window width was optimized using qualitative assessment of the resulting χ and Fourier transform.

The XANES spectra were transformed by taking the first derivative of the normalized spectra and smoothed using a smoothing function (Savitzky and Golay, 1964). Since the signal to noise level for the samples equilibrated at high *I* was low, the three samples were merged to improve the resolution of the data. This was deemed reasonable since the three spectra appeared identical in shape and magnitude of features.

Theoretical backscattering phase and amplitude functions for Cu-Cu backscatterers and Cu-O backscatterers were calculated using the *FEFF*8.0 code, with an input file based on a model of Tenorite (CuO) (generated with the program *WebATOMS* 1.4 (Ravel, 2001)). Functions for Cu-Al backscatterers were calculated by substituting an Al atom for a Cu atom in the second shell of the input file. During fitting, the value of the Debye Waller term (σ^2) for the second shell Cu backscatterer was fixed at 0.008 $Å^2$. Fixing the σ^2 reduced the number of free parameters in the fitting routine, and 0.008 $Å^2$ is consistent with the value used by other researchers to fit second-shell Cu sorption data (Cheah *et al.*, 1998, 2000; Farquhar *et al.*, 1996; Morton *et al.*, 2001). The edge shift (E_o) for all shells was constrained to be equal. An amplitude reduction factor (0.77) was determined by fitting the theoretical single scattering O and Cu shells to the same shells of the experimental spectra from well-characterized $Cu(OH)_2$ mineral (Sigma Chemicals). In all cases the number of independent variables in the fitting routine was less than the degrees of freedom (Stern, 1988). Absolute errors of the fitting results are 1% for bond distances, <20% for first-shell coordination numbers, and 25% for second-shell coordination numbers. Accuracies were verified by fitting well characterized reference materials ($Cu(OH)_2$ and CuO) and comparing the fitted bond distances and coordination numbers with XRD-derived structural parameters. Standard deviations estimated from the diagonal elements of the covariance matrix from the least-squares refinement were <1% for all varied parameters.

EPR spectroscopy experiments

Samples were prepared for electron paramagnetic resonance (EPR) spectroscopy experiments using the same procedures as described above for the XAFS spectroscopy experiments. The wet pastes were loaded into 1.1 mm O.D. × 0.9 mm I.D. clear fused-quartz cells and sealed with a polymer putty. Samples were analyzed at room temperature at a frequency of 9.387 GHz and microwave power of 2.0 mW using a Bruker Instruments ESP 300E spectrometer. A sweep of 2000 G centered at 2900 G was used for the EPR scans. Samples were scanned up to seven times to increase the signal to noise ratio. The scans were merged and centered for comparison. For presentation purposes, the ordinate scale on the graphs was varied; however, assuming the size of the free radical resonance (g_e) is consistent with the amount of sample in the microwave cavity, relative differences in peak height can be estimated from the graphs.

RESULTS

pH-edge results

Results from the pH-edge experiments are presented in Figure 1. For the low-*I* equilibrated samples there is little variation in sorption with pH. The large negative charge on the interlayer sites that is balanced with Na^+ can be displaced easily by divalent Cu^{2+} cations. This cation exchange is not pH dependent since the charge develops from isomorphic substitution and the ion attraction is electrostatic.

At high ionic strength, the increased concentration of background electrolyte cations (Ca^{2+}) out-compete Cu^{2+} for interlayer sites. As pH increased, sorption also increased until 100% of the Cu was removed from solution at pH 7. Note that at this pH the initial Cu solution was saturated with respect to CuO (s) which is the least soluble Cu mineral under the conditions of this experiment. However, it is unlikely that CuO (s) formed since the clay mineral was titrated from low pH where sorption occurred below saturation, reducing the Cu concentration before saturation was reached at the higher pH.

XANES results

Copper loading levels and final pH for the clay mineral samples are posted in Table 1. First derivatives of the K-edge XANES spectra from the samples and standards are presented in Figure 2. There are three unique features observed in the spectra that can be used to interpret local atomic structure of the Cu-clay complexes: (1) pre-edge features; (2) edge features; and (3) near-edge features. The pre-edge feature occurring at 8976 eV is due to a 1s–3d orbital transition that results from both octahedral and tetrahedral coordination. The existence of this peak is sensitive to a center of symmetry; the peak increases in intensity with distortions that remove the center of symmetry (Palladrino *et al.*, 1993; Xia *et al.*, 1997a). Similarity in the magnitude of the pre-edge peak in the XANES of the sorption samples to aqueous Cu indicates that the sorbed Cu has a distinct asymmetric first atomic shell similar to aqueous Cu.

In the XANES spectra there exist two peaks in the first derivative spectra between 8983 and 8992 eV that comprise the absorption edge. These peaks (labeled α and β) are a result of the main 1s–4p orbital transitions (Palladrino *et al.*, 1993; Xia *et al.*, 1997a). The splitting

https://doi.org/10.1346/CCMN.2004.0520307 Published online by Cambridge University Press

Table 1. Fitting results for Cu(II) sorbed on clay minerals and reference standards.

Sample	*I*	pH	Loading (mmol kg^{-1})	Cu-O shell			Cu-Cu shell			E_o (eV)
				R (Å)[a]	*N*[b]	σ^2 (Å^2)[c]	*R* (Å)	*N*	σ^2 (Å^2)[d]	
Montmorillonite										
	0.0001	4.01	59.1	1.96	4.51	0.005				3.97
	0.0001	5.49	108	1.96	4.27	0.004				1.68
	0.0001	5.90	96.1	1.95	4.19	0.004				2.37
	0.1	5.09	12.3	1.94	4.52	0.006	2.66	0.47	0.008	0.44
	0.1	5.61	12.2	1.94	4.48	0.005	2.63	0.60	0.008	0.44
	0.1	6.12	25.7	1.95	4.50	0.006	2.62	0.60	0.008	2.84
Beidellite										
	0.1	6.16	19.2	1.95	3.99	0.006	2.65	0.54	0.008	0.66
Standards										
$CuOH_2$				1.95	3.97	0.004	2.96	1.96	0.005	7.39
XRD[e]	equatorial			1.95 – 1.97	4.00		2.95	2.00		
	axial			2.36 – 2.92	2.00					
CuO				1.96	3.23	0.006	2.91	3.40	0.008	9.05
							3.10	3.02	0.008	
XRD[e]	equatorial			1.95 – 1.96	4.00		2.90	4.00		
							3.08	4.00		
	axial			2.78	2.00					
Cu acetate				1.95	3.24	0.004	2.61	0.84	0.008	5.08
XRD[e]	equatorial			1.95 – 1.99	4.00		2.62	1.00		
	axial			2.16	1.00					
Cu^{2+} (aq)				1.96	4.02	0.004				1.47
XAFS[f]	equatorial			1.97	4.00	0.004				
	axial			2.26	2.00	0.014				

[a] bond distances; [b] coordination number; [c] Debye Waller factor; [d] fixed; [e] from Cheah *et al*. (2000); [f] from Ozutsumi *et al*. (1991)

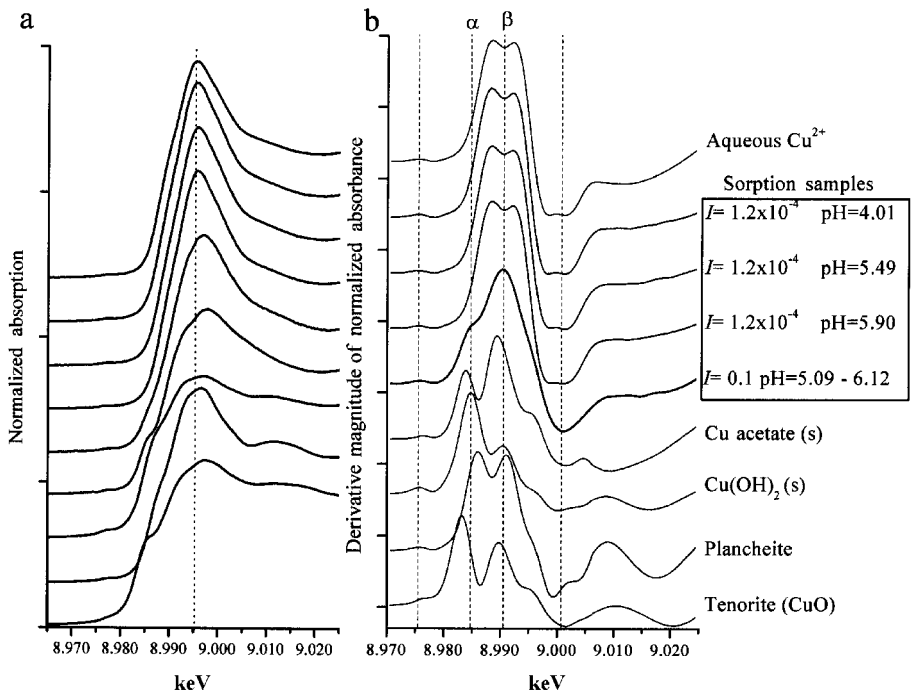


Figure 2. (a) XANES and (b) first derivative of XANES of Cu sorbed onto montmorillonite and selected reference materials. Vertical dashed lines are aligned with peaks of interest. $I = 0.1$ XANES is an average of three different samples (see text).

https://doi.org/10.1346/CCMN.2004.0520307 Published online by Cambridge University Press

of the main K-edge absorption peak is the subject of debate. Kau *et al.* (1987) reported that with increasing covalency there is an increased intensity of the α peak between 8983 and 8985 eV. The cause of this decreased excitation energy is reported to be a result of either the decrease in p-orbital energy that arises from the sharing of metal-d electrons with ligands (Kau *et al.*, 1987), or a change in the axial-bond distances upon covalent bonding and the resulting multiple scattering off of the axial ligands (Palladrino, 1993). The decreased energy of the α peak is consistent with Cu complexes that have covalent character. Specifically, the features at 8985 eV and 8990 eV in the high-*I* samples are directly in line with the features in the $Cu(OH)_2$ mineral. However, the peak intensities in the high-*I* samples are different than in $Cu(OH)_2$ (s), indicating that the local atomic structure or size of the sorption complexes is different. In the samples equilibrated at low *I* both α and β peaks are in the same positions as Cu (aq), suggesting that the sorbed Cu(II) retains its hydration sphere.

In the first oscillations directly following the edge (near edge), the shape and features in the spectra are influenced by the local atomic structure surrounding the central absorber atom. The near-edge features in the low-*I* equilibrated samples are nearly identical to aqueous Cu^{2+}. The near-edge features in the high-*I* equilibrated samples are distinctly different from the low-*I* equilibrated samples, and are similar in energy position to $Cu(OH)_2$ (s). However, as with the edge features, there are distinct differences in the near-edge features between the high-*I* samples and the $Cu(OH)_2$ mineral, again suggesting that the local atomic structure of sorbed Cu is different from the local atomic structure of Cu in $Cu(OH)_2$ (s). The dissimilarities between the XANES features in the Cu sorbed samples and the tenorite and plancheite XANES features suggest that the sorbed Cu complexes are not forming phases with similar local atomic structure as these minerals.

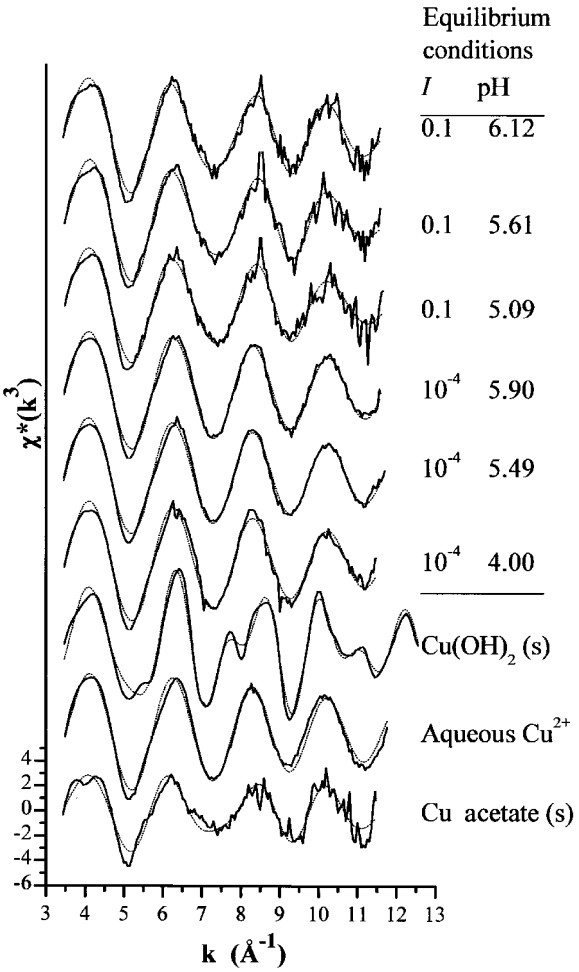


Figure 3. k^3 weighted χ spectra of Cu sorbed on montmorillonite samples at different pH and ionic strengths. The amount of Cu sorbed on each sample is listed in Table 1. Three reference mineral spectra are also included for comparison of features. The dashed lines are best fits of data.

EXAFS results

The k^3-weighted EXAFS spectra for the Cu-sorbed clay minerals and select standards are presented in Figure 3. In all of the clay mineral samples, the spectra are dominated by a single sinusoidal wave resulting from backscattering off of O atoms in the first atomic shell. In the samples incubated at high *I* there is a small shoulder present at the beginning of the first oscillation peak. This feature is not present in the aqueous copper standard nor the clay samples equilibrated at low *I*, yet is present in the $Cu(OH)_2$ mineral spectra.

To isolate atomic-shell contributions further, the χ spectra were Fourier transformed. The modulus of the FT are presented in Figure 4. The first peak in the FT spectra centered at 1.5 Å is indicative of O back-scattering atoms. In the clay-mineral samples equilibrated at high *I* there exists a second peak in the FT spectra centered at 2.2 Å that is due to backscattering from a second-neighbor atomic shell. Figure 5 shows the intensity of this peak relative to the hydrated copper sorbed at low *I*. Peaks further out in the clay-mineral FT spectra are too small to identify with any confidence; however, they are probably due to multiple-scattering effects (Cheah *et al.*, 1998, 2000; Farquhar *et al.*, 1996), as well as backscattering structural atoms from the montmorillonite mineral. The position of the second peak matches that of the Cu-Cu backscattering peak in Cu acetate, and has a decreased R-space position as compared to the Cu-Cu backscatterer observed in the mineral $Cu(OH)_2$ (Δ ~0.32 Å). Thus, the FT modulus in the high-*I* samples suggests that the local atomic structure of the complexes formed on the clay minerals is different from that of $Cu(OH)_2$ (s). Both montmorillonite and beidellite have similar features, suggesting that the complexation mechanism is the same in the two smectite minerals. At low *I* there were no significant

https://doi.org/10.1346/CCMN.2004.0520307 Published online by Cambridge University Press

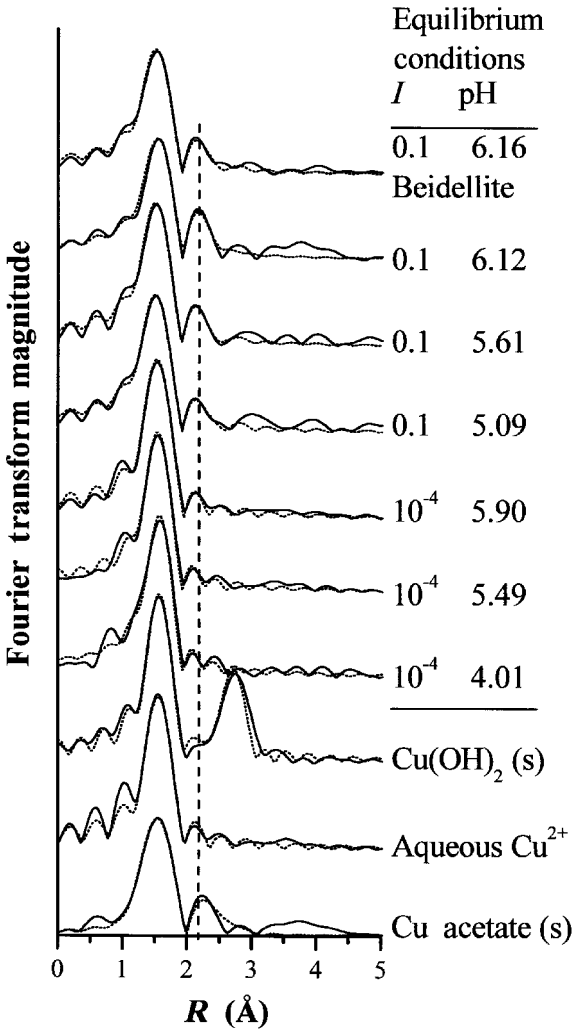


Figure 4. Fourier transform modulus and best fits for Cu sorbed on montmorillonite and beidellite samples at different pH and ionic strengths. The amount of Cu sorbed on each sample is listed in Table 1. Three reference mineral spectra are also included for comparison of features. The dashed lines are best fits of data. The parameters used in fitting are reported in Table 1.

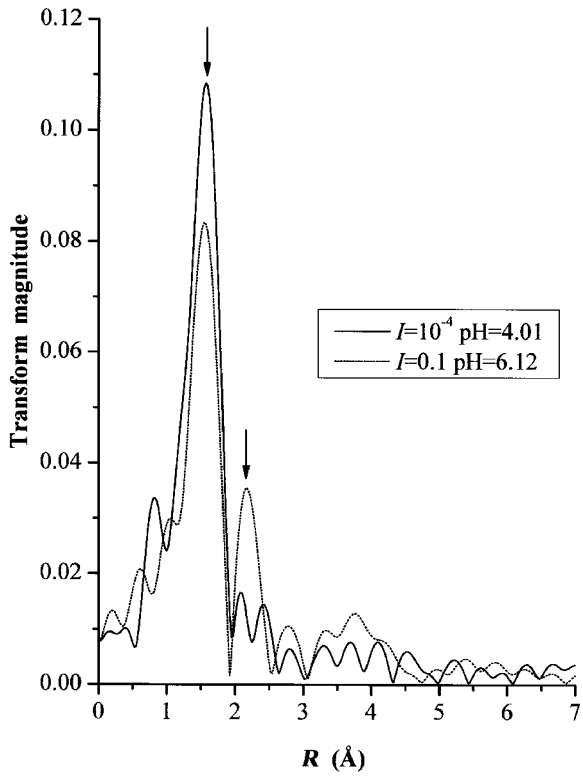


Figure 5. Fourier transform modulus for Cu sorbed on montmorillonite at pH = 6.12 and high ionic strength, and pH = 4.01 and low ionic strength ($\Delta k = 3.4 - 11.8$ Å^{-1}). Samples are plotted on the same ordinate scale to illustrate the magnitude of second-shell backscattering contributions. The arrows indicate first- and second-shell backscattering features.

second-shell peaks observed in the FT spectra, indicating that the local atomic environment surrounding the Cu consist of a single shell with a similar coordination environment as aqueous Cu.

The fitting results are listed in Table 1. For the low-*I* samples, only a single backscattering O shell consisting of ~4 O atoms at a bond distance of 1.94 Å was fit. This local atomic shell is consistent with the coordination observed in the aqueous Cu standard, and has been observed by other researchers (Morton *et al.*, 2001). The axial-O atoms could be fit only if two shells were used and the coordination number was fixed. However, the axial O shell was not fit in this study as it does not provide any additional information. This is consistent with the fitting approach used to fit both model compounds and Cu sorbed on mineral surfaces (Cheah *et al.*, 2000; Farquhar *et al.*, 1996; Morton *et al.*, 2001).

For the samples equilibrated at high *I*, two atomic shells were fit. One of the shells consisted of ~4 O atoms at 1.95 Å, and the other consisted of a Cu atom with an average bond distance of 2.64 Å. The O-bond distances are similar to those observed in hydrated Cu^{2+} and many covalently bonded Cu molecules (Cheah *et al.*, 2000; Kau *et al.*, 1987; Palladrino *et al.*, 1993). However, the Cu–Cu bond distances are significantly shorter than the Cu–Cu bond distances observed in copper oxides and hydroxides (2.95 Å). The possibility that the second shell fit consisted of a structural atom such as Si or Al from the clay mineral was tested. Based on the poor fit in the RSF and investigation of the back transform (Figure 6), it was concluded that the second shell in the EXAFS spectra was a Cu atom. Figure 6 shows the back transformed second shell and the respective fit using Cu and Al second-shell backscatterers. The fit of the second shell with a Cu atom resulted in a lower residual (residual = 19) than fitting the second shell with an Al atom (residual = 38). In addition, fitting with the Cu second-shell backscatterer resulted in bond distance and coordination numbers that were consistent with the RSF and k-space fitting results, while results from fitting with an Al backscatterer were inconsistent.

https://doi.org/10.1346/CCMN.2004.0520307 Published online by Cambridge University Press

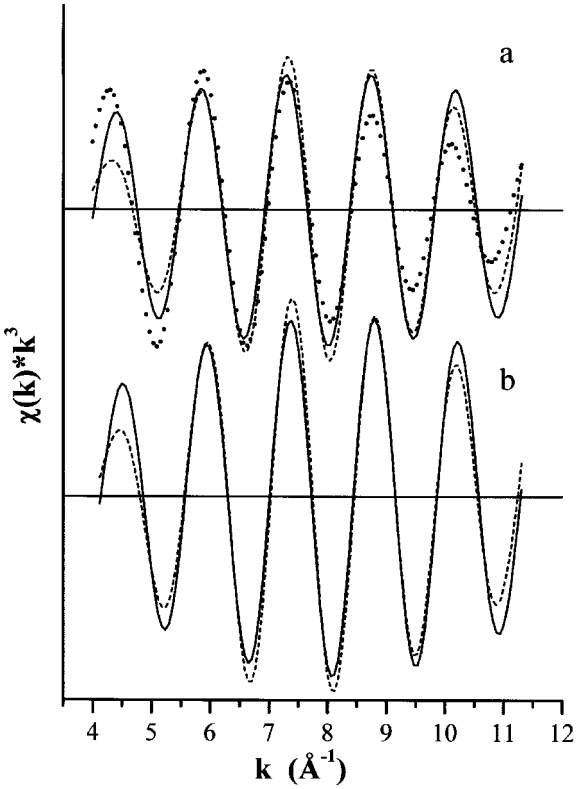


Figure 6. Backtransforms (ΔR = 1.9–2.5 Å) of (a) second shell in Fourier transform modulus of montmorillonite sample incubated at I = 0.1 pH = 6.12, and (b) Cu acetate sample. The dashed lines are best fits using a single Cu backscatterer atom and the dotted line in panel a is best fit using a single Al backscatterer atom.

Copper acetate, which has a Cu-Cu backscatterer at 2.62 Å was used to further investigate the spectral features and contributions in the EXAFS spectra from a short Cu-Cu backscattering pair. Peak position in the RSF (Figure 4) and back-transform oscillations (Figure 6) for the Cu-Cu backscatterer in Cu acetate and the high-I sorption samples are identical, providing further evidence that the second-shell backscatterer in the samples equilibrated at high I is Cu and not structural Al or Si from the clay mineral. The average coordination number for the second shell is 0.55. This low coordination is indicative of small molecular units with minimal backscattering amplitude (Cheah *et al.*, 1998; Farquhar *et al.*, 1996), and is affected by the inherent error in coordination number derived from fitting second-shell backscatterers (±25%). Fitting the model compound Cu acetate, which is a dimer, also gave a coordination number <1 (0.84). Another explanation for the low coordination number may be that the EXAFS spectra represent an average of all Cu in the sample. Therefore, some of the Cu may exist as monomers and thus dilute the overall coordination number obtained from fitting. Thus, the EXAFS spectroscopy data reveal that at high I, Cu is sorbing as complexes coordinated by ~4 O atoms in the first atomic shell and ~1 Cu atom in the second atomic shell. This is in agreement with the XANES spectra.

Attempts to fit an Al or Si atom as a third atomic backscatterer from the montmorillonite samples equilibrated at high I were successful, yielding 0.44 Al or Si atoms at 3.03 Å (fit not shown). However, the contribution of this backscatterer to the overall spectra was <5%, leading to poor confidence in the fit results. Such a small contribution to the overall spectra is not surprising since not all the Cu atoms are coordinated to the mineral in multi-nuclear sorption, and Si or Al atomic shells that are >3 Å away would be weak backscatterers, thus making XAFS contributions difficult to measure.

EPR results

Spectra from the EPR experiments are presented in Figure 7. An isotropic absorption line at g = 2.184 is present in the spectrum for the aqueous copper nitrate sample. Because of the free tumbling of the hydrated Cu cation, the hyperfine coupling constants are averaged, resulting in a single isotropic resonance (Clementz *et al.*, 1973; Hyun *et al.*, 2000). Similarly, the spectrum for the montmorillonite sample equilibrated with Cu at low I also shows an isotropic resonance at g = 2.184, suggesting that the adsorbed Cu has a coordination environment similar to that of aqueous Cu^{2+}. The free tumbling of the adsorbed Cu indicates that the atom is unrestricted by the adsorption forces from the permanent charge on the montmorillonite, and that there are several layers of water in the interlayer. In contrast, spectra for the samples equilibrated at high I yield only a small resonance feature at g = 2.003, which is the free-radical resonance commonly present in clay minerals (Clementz *et al.*, 1973) and is shown in the hydrated montmorillonite blank in Figure 7. The loss of Cu-derived resonance features in spectra for the high-I equilibrated samples probably occurs because of dipolar and spin interactions between Cu atoms in multinuclear complexes (Hyun *et al.*, 2000; McBride, 1982a; Weesner and Bleam, 1997; Xia *et al.*, 1997b). The absence of these features does not indicate inner-sphere sorption, because Cu adsorbed as inner-sphere complexes on Al oxide has a distinct anisotropic rigid limit of $g_{\perp}$ ~2.07 and $g_{\parallel}$ = 2.35 with A_2 = 155 gauss (Martinez and McBride, 2000; McBride *et al.*, 1984). The EPR spectra for the high-I samples thus suggest that Cu is not sorbed by inner-sphere complexation, but instead exists as multinuclear complexes. This sorption mechanism is consistent with the EXAFS results.

DISCUSSION

Sorption as a function of pH

Bradbury and Baeyens (1999) modeled proton sorption on clay-mineral edges using two types of surface hydroxyl groups, each capable of taking a positive,

https://doi.org/10.1346/CCMN.2004.0520307 Published online by Cambridge University Press

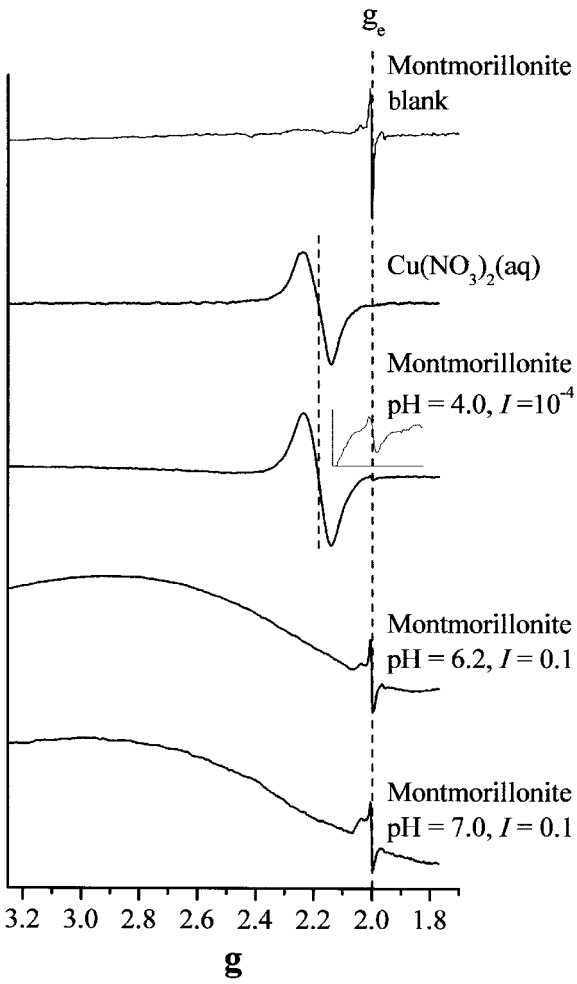


Figure 7. EPR spectra of Cu sorbed on montmorillonite as a function of pH and ionic strength. g_e is the free electron resonance at 2.003. A montmorillonite blank sample (no Cu) and aqueous Cu^{2+} EPR spectra are shown for reference. Inset on montmorillonite is zoomed in to show features since ordinate scales are different for each spectra.

negative or zero charge. The first type of hydroxyl was said to have a strong affinity for metal cations and the second was described as a site with a much weaker affinity (Bradbury and Baeyens, 1999). Stadler and Schindler (1993) suggested that the silanol groups on the edge sites are acids that can dissociate protons becoming negatively charged, but can only form electrostatic bonds with cations, and that the aluminol groups can be either proton acceptors or donors capable of forming covalent bonds with metal cations. This description is analogous to the weak and strong affinity hydroxyl functional groups that Bradbury and Baeyens (1999) fit in their model. In the high-*I* equilibrated system we observed a distinct increase in sorption as a function of pH. This behavior is a classical pH edge that suggests sorption on hydroxyl functional groups. Subtracting the 20% of absorption which occurs as non-pH dependent sorption (Figure 1 shows that ~20% of the Cu sorbed is non-pH dependent), the midpoint of the pH edge occurs at pH = 5.7. Farrah and Pickering (1976) titrated Cu montmorillonite suspensions and found that the midpoint occurred at ~6.1. Stadler and Schindler (1993) observed a midpoint at pH 5.8 using similar equilibrium conditions to those in our study (*i.e.* Cu on montmorillonite at I = 0.1 M, solid-solution = 0.01, initial [Cu] = 1×10^{-4} M). Stadler and Schindler (1993) did not have 20% permanent charge difference, but instead observed and modeled ~10% permanent charge difference. The differences may be a result of clay treatment and the higher initial Cu concentration.

Based on the above discussion, one may interpret the behavior of Cu sorption observed in the pH edge to be a result of sorption of Cu on aluminol functional groups. Fitting a two-site sorption model, Stadler and Schindler (1993) proposed that the predominant Cu sorption mechanism under high-*I* equilibration is a monodentate $CuOH^+$ complex with structural AlO^- functional groups. Undabeytia *et al.* (2002) modeled Cu^{2+} sorption on montmorillonite using a two-site model that included planar and edge sorption. They found that the Cu sorption maximum for the edge sites was ~22 mmol kg^{-1}, which is similar to the aluminol edge-site capacity of 22.4 mmol kg^{-1} reported by Zachara and Mckinley (1993) who based their value on particle diameter, structural formula and crystallographic dimensions. Modeling sorption data clearly shows the importance of edge-site sorption, but these models usually neglect multinuclear complexation. Results from our molecular-level experiments show that multinuclear Cu complexation is the predominant sorption mode at high *I*.

Surface complexation mechanism

Copper has been reported to occur in four common dimer configurations (Cheah *et al.*, 1998). Based on similarities in bond distances and XANES features, Cheah *et al.* (1998) proposed that Cu-dimer complexes formed on the surface of silicon dioxide had a structural configuration similar to Cu acetate, composed of two square pyramids linked by a weak metal–metal bond along the axial direction. Multinuclear hydrolysis complexes with the formula $Cu_2(OH)_2^{2+}$ (aq) are the most common aqueous hydrolysis products (Baes and Mesmer, 1986); however, calculations reveal that $Cu_2(OH)_2^{2+}$ (aq) is <1% of the total Cu in our initial solutions and $Cu(OH)^+$ (aq) comprises 1.5%. The Cu–Cu distance in $Cu_2(OH)_2^{2+}$ (aq) should be similar to the $Cu(OH)_2$ (s) (Cheah *et al.*, 1998) which is at least 0.3 Å longer than the bond distances observed in this study. The minerals shattuckite and plancheite consist of Cu oxide trioctahedral layers sandwiched between two silicon tetrahedra chains arranged in a non-continuous sheet (Evans and Mrose, 1977). The chain silicate sheets are adjoined to adjacent Si tetrahedral sheets and chains by ribbons of four-fold coordinated Cu atoms that edge-

https://doi.org/10.1346/CCMN.2004.0520307 Published online by Cambridge University Press

share O ligands. These ribbons have similar structural configurations to the Cu–Cu bonds in the $Cu(OH)_2$ (s). However, unlike $Cu(OH)_2$ (s), which has Cu–Cu separations of 2.95 Å, the Cu ribbons in shattuckite and plancheite are 2.64 Å apart (Farquhar *et al.*, 1996). The shorter distance in the Cu ribbons is due to the structural confinements imposed by attachment to the tetrahedral-Si chains. The Cu dimers on montmorillonite may be attached on several locations on the edge of the montmorillonite that creates a structural confinement analogous to the Cu ribbons in shattuckite or plancheite, thus allowing for similar short Cu–Cu separations.

Further evidence for the formation of the Cu dimers instead of monomers is provided by comparing the second derivative XANES spectra of our samples with those of Cheah *et al.* (1998) (Figure 8). The results of Cheah *et al.* (1998) showed that Cu sorbed on amorphous SiO_2 at loading levels of 6–10 mmol kg^{-1} existed as multinuclear-dimer complexes, while Cu sorbed on Al_2O_3 under the same equilibrium conditions existed as inner-sphere mononuclear complexes. The inner-sphere complexation mechanism was based on the fitting of the second peak in the Fourier transform with an Al atom located 2.83 Å away from the Cu atom, as well as a distinct decrease in the position of the maximum amplitude peak in the back transformed second peak, which is consistent with lighter backscatterers (Cheah *et al.*, 1998).

The work of Morton *et al.* (2001) showed that Cu forms a multinuclear precipitate on the surface of montmorillonite with a structural arrangement similar to the $Cu(OH)_2$ mineral, *i.e.* Cu–Cu separations of ~2.98 Å. The Cu loading in the study of Morton *et al.* (2001) ranged from 40 to 97 mmol kg^{-1}, which is several times the loading level in our samples incubated at high *I*. In addition, in the suspensions in which significant Cu backscatterers were observed at 2.98 Å, the initial Cu concentration was saturated with respect to CuO (s), yet undersaturated with respect to $Cu(OH)_2$ (s). Cheah *et al.* (2000) performed experiments of Cu loading on amorphous SiO_2 using loading levels ranging from 112 to 146 mmol kg^{-1} and showed that at these higher sorption levels (as compared with their previous study (Cheah *et al.*, 1998)), the Cu sorption complexes were multinuclear complexes with similar local atomic structure as $Cu(OH)_2$ (s). Xia *et al.* (1997b) also found that Cu sorbed to SiO_2 (s) as multinuclear complexes similar to the $Cu(OH)_2$ mineral. In the experiments of Cheah *et al.* (2000) and Xia *et al.* (1997b), the initial solutions were undersaturated with respect to CuO (s) or $Cu(OH)_2$ (s). Thus, we speculate that the differences between our results and those of Morton *et al.* (2001) are due to loading level.

Farquhar *et al.* (1996) suggested that the Cu dimers were sorbing by an inner-sphere complexation mechanism on the basal planes of the muscovite. In our study, complexation on the basal plane seems unlikely since the basal-oxygen atoms are completely coordinated in an ideal montmorillonite structure. Adsorption on the basal plane of the montmorillonite occurs predominantly through coulombic forces, and because the concentration of Ca is $>10^3$ times the Cu concentration, mass action dictates that Ca would out-compete Cu for the basal-plane adsorption sites. The higher hydration energy of Ca over Cu suggests that Ca is unlikely to form inner-sphere complexes with the ligands at the steps, kinks and edges of the montmorillonite, while Cu can adsorb to these sites by inner-sphere complexation. Thus, we hypothesize that Cu is sorbing as dimers on silanol or aluminol functional groups that have incomplete coordination. Farquhar *et al.* (1996) sorbed Cu complexes on muscovite and reported that Si atoms could be fit as a third shell at ~3.25 Å. In our study the results indicate that bond distances between the Cu and the structural Si and Al atoms are probably near 3.05 Å, which is consistent with Cu forming a corner-sharing bond with the structural ligands (Cheah *et al.*, 1998).

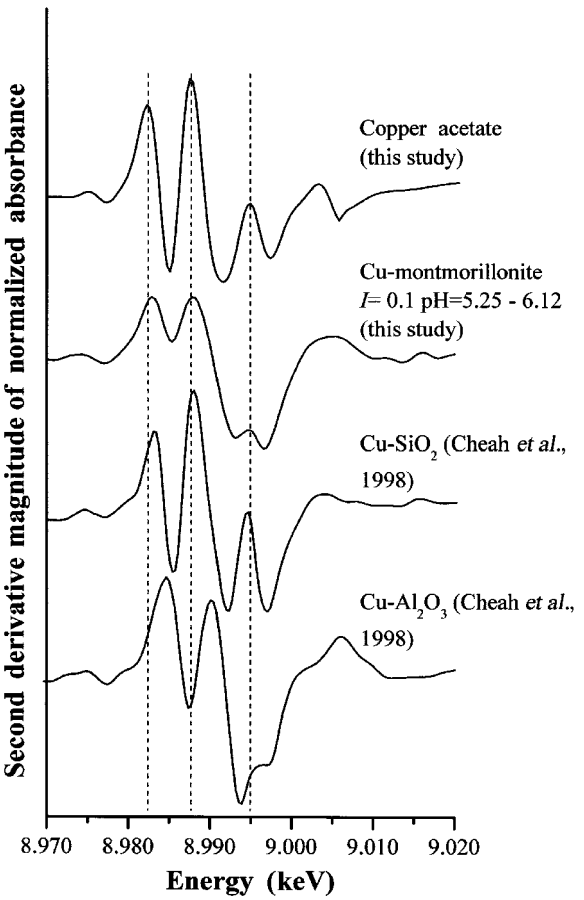


Figure 8. Comparison of second-derivative spectra from montmorillonite samples incubated at high *I* averaged (see text) with results from Cu sorbed on amorphous SiO_2 and Al_2O_3 as reported by Cheah *et al.* (1998). The Cu acetate spectrum was used to correlate the energy of the samples in the two studies.

https://doi.org/10.1346/CCMN.2004.0520307 Published online by Cambridge University Press

An example of Cu complexation mechanism on smectite minerals is illustrated in Figure 9. Formation of small metal multinuclear clusters have been proposed as precursors for the formation of more extensive precipitates (Cheah *et al.*, 1998; Farquhar *et al.*, 1996; Schlegel *et al.*, 2001). CuO (s) has the lowest solubility followed by $Cu(OH)_2$ (s) (Baes and Mesmer, 1986). Precipitation from solution usually starts with $Cu(OH)_2$ (s) as a result of reaction kinetics (Cheah *et al.*, 1998). The $Cu(OH)_2$ (s) may then ripen to the more stable CuO phase if conditions are favorable. One can envision a similar process occurring for the Cu-Cu dimers observed on the surface of the clay minerals used in this study. However, the results from two separate samples (data not shown) aged for 1 week showed no significant differences from the montmorillonite samples incubated for this study. If the Cu dimers were to convert to $Cu(OH)_2$ (s) or CuO (s) complexes, it would require significant rearrangement of the structure (Cheah *et al.*, 1998). Thus, we propose that the Cu-Cu dimers sorbing onto the surface are stable complexes. $Cu(OH)_2$ precipitates on the surface of montmorillonite as observed by Morton *et al.* (2001) appear to occur as a result of higher Cu loadings, possibly created from multi-layer sorption on the edge sites.

CONCLUSIONS

Macroscopic experiments were used to show that Cu had distinct uptake behavior as a function of ionic strength and interlayer cations on montmorillonite. We incubated our samples below the saturation indices for CuO (s) and $Cu(OH)_2$ (s), and used XAFS and EPR spectroscopies to show that Cu sorption on montmorillonite under high-*I* conditions sorbs as Cu-Cu dimers. These results are consistent with the results observed by Cheah (1998) and Farquhar (1996) for sorption of Cu at low loading levels on SiO_2 (s) and muscovite, respectively, and are in contrast to the $Cu(OH)_2$-like complexes sorbed on montmorillonite (Morton *et al.*, 2001) and SiO_2 (s) (Cheah *et al.*, 2000) when loading levels are high. It appears that Cu does not form surface precipitates having the 2:1 layer silicate structure as observed for Ni, Co and Zn (Dahn *et al.*, 2002; Schlegel *et al.*, 1999, 2001). This is probably due to the Jahn-Teller distortion that creates an unfavorable energy when Cu is substituted in a symmetric octahedral environment (Burns, 1970).

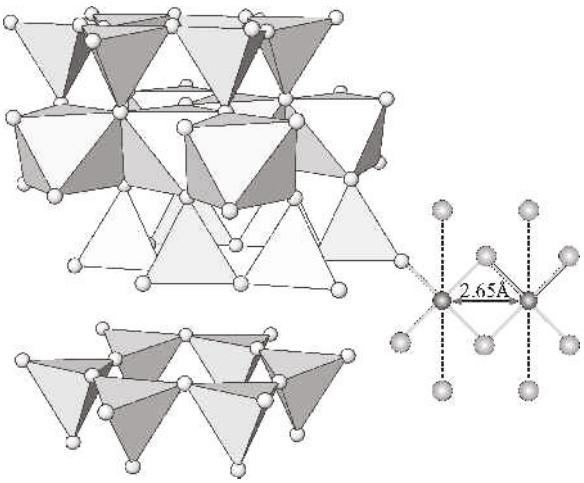


Figure 9. Illustration depicting possible Cu complexation mechanisms on smectite clays based on results from this study.

Results from the beidellite sample indicate that the Cu sorption complex is the same as Cu sorption on montmorillonite. This suggests that the small degree of tetrahedral substitution in beidellite is not enough to induce formation of basal plane-sorbed Cu complexes similar to those observed by Farquhar *et al.* (1996) on muscovite.

ACKNOWLEDGMENTS

Support for this research was provided by a National Research Initiative-USDA grant. Portions of this research were carried out at the Stanford Synchrotron Radiation Laboratory (SSRL), a national user facility operated by Stanford University on behalf of the US Department of Energy, Office of Basic Energy Sciences. The SSRL Structural Molecular Biology Program is supported by the Department of Energy, Office of Biological and Environmental Research, and by the National Institutes of Health, National Center for Research Resources, Biomedical Technology Program. A portion of the research described in this paper was performed in the Environmental Molecular Sciences Laboratory, a national scientific user facility sponsored by the Department of Energy's Office of Biological and Environmental Research and located at the Pacific Northwest National Laboratory (PNNL). The PNNL is operated for DOE by Battelle Memorial Institute under contract DE-AC06-76RL0 1830. D. Strawn is grateful to Glenn Waychunas, Mickey Gunter and the staff at SSRL for discussions on experimental details. Reviewers' comments and edits are also greatly appreciated.

REFERENCES

Ankudinov, A.L., Ravel, B., Rehr, J.J. and Conradson, S.D. (1998) Real space multiple scattering calculation of XANES. *Physical Review B*, **58**, 7565.

Baes, C.F. and Mesmer, R.E. (1986) *The Hydrolysis of Cations*. Krieger Publishing Co., Malabar, Florida.

Bradbury, M.H. and Baeyens, B. (1999) Modelling the sorption of Zn and Ni on Ca-montmorillonite. *Geochimica et Cosmochimica Acta*, **63**, 325–326.

Burns, R.G. (1970) *Mineralogical Applications of Crystal Field Theory*. Cambridge University Press, Cambridge, UK.

Cheah, S.-F., Brown, G.E., Jr. and Parks, G.A. (1998) XAFS spectroscopy study of Cu(II) sorption on amorphous SiO_2 and γ-Al_2O_3: Effect of substrate and time on sorption complexes. *Journal of Colloid and Interface Science*, **208**, 110–128.

Cheah, S.-F., Brown, G.E., Jr. and Parks, G.A. (2000) XAFS study of Cu model compounds and Cu^{2+} sorption on amorphous SiO_2, γ-Al_2O_3, and anatase. *American Mineralogist*, **85**, 118–132.

https://doi.org/10.1346/CCMN.2004.0520307 Published online by Cambridge University Press

Clementz, D.M., Pinnavaia, T.J. and Mortland, M.M. (1973) Stereochemistry of hydrated copper(II) ions on the interlamellar surfaces of layer silicates. An electron spin resonance study. *The Journal of Physical Chemistry*, **77**, 196–200.

Dahn, R., Scheidegger, A.M., Manceau, A., Schlegel, M., Baeyens, B., Bradbury, M.H. and Morales, M. (2002) Neoformation of Ni phyllosilicate upon Ni uptake on montmorillonite: A kinetic study by powder and polarized extended X-ray absorption fine strucuture spectroscopy. *Geochimica et Cosmochimica Acta*, **66**, 2335–2347.

Dahn, R., Scheidegger, A.M., Manceau, A., Schlegel, M.L., Baeyens, B., Bradbury, M.H. and Chateigner, D. (2003) Structural evidence for the sorption of Ni(II) atoms on the edges of montmorillonite clay minerals: A polarized X-ray absorption fine structure study. *Geochimica et Cosmochimica Acta*, **67**, 1–15.

Di Leo, P. and O'Brien, P. (1999) Nuclear magnetic resonance (NMR) study of Cd^{2+} sorption on montmorillonite. *Clays and Clay Minerals*, **47**, 761–768.

Evans, H.T. and Mrose, M.E. (1977) The crystal chemistry of the hydrous copper silicates, shattuckite and plancheite. *American Mineralogist*, **62**, 491–502.

Farquhar, M.L., Charnock, J.M., England, K.E.R. and Vaughan, D.J. (1996) Adsorption of Cu(II) on the (0001) plane of mica: A REFLEXAFS and XPS study. *Journal of Colloid and Interface Science*, **177**, 561–567.

Farrah, H. and Pickering, W.F. (1976) The sorption of copper species. *Australian Journal of Chemistry*, **1976**(29), 1167–1176.

Ford, R.G. and Sparks, D.L. (1998) The potential formation of secondary hydrotalcite-like precipitates during Zn and Cu sorption to pyrophyllite. *Mineralogical Magazine*, **62A**, 462–463.

Helmy, A.K., Ferreiro, E.A. and deBussetti, S.G. (1994) Cation exchange capacity and condition of zero charge of hydroxyl-Al montmorillonite. *Clays and Clay Minerals*, **42**, 444–450.

Hyun, S.P., Cho, Y.H., Kim, S.J. and Hahn, P.S. (2000) Cu(II) sorption mechanisms on montmorillonite: An electron paramagnetic resonance study. *Journal of Colloid and Interface Science*, **222**, 254–261.

Kau, L.S., Spira-Solomon, D.J., Penner-Hahn, J.E., Hodgson, K.O. and Solomon, E.I. (1987) X-ray absorption edge determination of the oxidation state and coordination number of copper: Application to the Type 3 site in Rhus vernicifera Laccase and its reaction with oxygen. *Journal of the American Chemical Society*, **109**, 6433–6442.

Lytle, F.W., Greegor, R.B., Sandstrom, D.R., Marques, E.C., Wong, J., Spiro, C.L., Huffman, G.P. and Huggins, F.E. (1984) *Nuclear Instrumental Methods*, **226**, 542–548.

Marshal, C.E. (1935) Layer lattices and the base exchange clays. *Zeitschrift für Kristallographie und Mineralogie*, **91**, 443–449.

Martinez, C.E. and McBride, M.B. (2000) Aging of coprecipitated Cu in alumina: Changes in structural location, chemical form, and solubility. *Geochimica et Cosmochimica Acta*, **64**, 1729–1736.

McBride, M.B. (1982a) Cu^{2+} sorption characteristics of aluminum hydroxide and oxyhydroxides. *Clays and Clay Minerals*, **30**, 21–28.

McBride, M.B. (1982b) Hydrolysis and dehydration reactions of exchangeable Cu^{2+} on hectorite. *Clays and Clay Minerals*, **30**, 200–206.

McBride, M.B. and Bouldin, D.R. (1984) Long-term reactions of copper(II) in a contaminated calcareous soil. *Soil Science Society of America Journal*, **48**, 56–59.

McBride, M.B., Fraser, A.R. and McHardy, W.J. (1984) Cu^{2+} interaction with microcyrstalline gibbsite. Evidence for oriented chemisorbed copper ions. *Clays and Clay Minerals*, **32**, 12–18.

Morton, J.D., Semrau, J.D. and Hayes, K.F. (2001) An X-ray absorption spectroscopy study of the structure and reversibility of copper adsorbed on montmorillonite clay. *Geochimica et Cosmochimica Acta*, **65**, 2709–2722.

O'Day, P., Brown, G.E., Jr. and Parks, G.A. (1994) X-ray absorption spectroscopy of cobalt (II) multinuclear surface complexes and surface precipitates on kaolinite. *Journal of Colloid and Interface Science*, **165**, 269–289.

Ozutsumi, K., Miyata, Y. and Kawashima, T. (1991) EXAFS and spectrophotometric studies on the structure of Mono and Bis(Aminocarboxylato) copper(II) complexes in aqueous solution. *Journal of Inorganic Biochemistry*, **1991**(44), 97–108.

Palladrino, L., Della Long, S., Reale, A., Belli, M., Scafati, A., Onori, G. and Santucci, A. (1993) X-ray absorption near edge structure (XANES) of Cu(II)-ATP and related compounds in solution: Quantitative determination of the distortion of the Cu site. *Journal of Physical Chemistry*, **98**, 2720–2726.

Papelis, C. and Hayes, K.F. (1996) Distinguishing between interlayer and external sorption sites of clay minerals using X-ray absorption spectroscopy. *Colloids and Surfaces*, **107**, 89.

Ravel, B. (2001) ATOMS: crystallography for the X-ray absorption spectroscopist. *Journal of Synchrotron Radiation*, **8,** 314–316.

Ressler, T. (1998) *WinXAS*: A program for X-ray absorption spectroscopy data analysis under MS-Windows. *Journal of Synchrotron Radiation*, **5**, 118–122.

Savitzky, A. and Golay, M.J.E. (1964) Smoothing and differentiation of data by simplified least squares procedures. *Analytical Chemistry*, **36**, 1627–1639.

Schecher, W. (1998) *Mineql+* version 4.5. Environmental Research Software, Hallowell, Maine, USA.

Schindler, P.W., Liechti, P. and Westall, J.C. (1987) Adsorption of copper, cadmium and lead from aqueous solution to the kaolinite/water interface. *Netherlands Journal of Agricultural Science*, **35**, 219–230.

Schlegel, M.L., Manceau, A., Chateigner, D. and Charlet, L. (1999) Sorption of metal ions on clay minerals I. Polarized EXAFS evidence for the adsorption of Co on the edges of hectorite particles. *Journal of Colloid and Interface Science*, **215**, 140–158.

Schlegel, M., Manceau, A., Charlet, L., Chatigner, D. and Hazemann, J. (2001) Sorption of metal ions on clay minerals. III. Nucleation and epitaxial growth of Zn phyllosilicate on the edge of hectorite. *Geochimica et Cosmochimica Acta*, **65**, 4155–4170.

Sposito, G. (1989) *The Chemistry of Soils*. Oxford University Press, Inc., New York.

Stadler, M. and Schindler, P.W. (1993) Modeling of H^+ and Cu^{2+} adsorption on calcium-montmorillonite. *Clays and Clay Minerals*, **41**, 288–296.

Stern, E.A. (1988) Theory of EXAFS. Pp. 3–51 in: *X-ray Absorption: Principles, Applications, and Techniques of EXAFS, SEXAFS, and XANES* (D.C. Koningsberger and R. Prins, editors) Wiley, New York.

Strawn, D.G. and Sparks, D.L. (1999) The use of XAFS to distinguish between inner- and outer-sphere lead adsorption complexes on montmorillonite. *Journal of Colloid and Interface Science*, **216**, 257–269.

Towle, S.N., Bargar, J.R., Brown, G.E., Jr. and Parks, G.A. (1997) Surface precipitation of Co(II)(aq) on Al_2O_3. *Journal of Colloid and Interface Science*, **187**, 62–82.

Undabeytia, T., Nir, S., Rytwo, G., Sereban, C., Morillo, E. and Maqueda, C. (2002) Modeling adsorption-desorption processes of Cu on edge and planar sites of montmorillonite. *Environmental Science and Technology*, **36**, 2677–2683.

https://doi.org/10.1346/CCMN.2004.0520307 Published online by Cambridge University Press

Weesner, F.J. and Bleam, W.F. (1997) X-ray absorption and EPR spectroscopic characterization of the adsorbed copper(II) complexes at the boehmite (AlOOH) surface. *Journal of Colloid and Interface Science*, **196**, 79–86.

Xia, K., Bleam, W. and Helmke, P.A. (1997a) Studies of the nature of Cu^{2+} and Pb^{2+} binding sites in soil humic substances using X-ray absorption spectroscopy. *Geochimica et Cosmochimica Acta*, **61**, 2211–2221.

Xia, K., Mehadi, A., Taylor, R.W. and Bleam, W.F. (1997b) X-ray absorption and electron paramagnetic resonance studies of Cu(II) sorbed to silica: Surface-induced precipitation at low surface coverages. *Journal of Colloid and Interface Science*, **185**, 252–257.

Zachara, J.M. and McKinley, J.P. (1993) Influences of hydrolysis on the sorption of metal cations by smectites: Importance of edge coordination reactions. *Aquatic Sciences*, **55**, 1015–1621.

Zachara, J.M., Smith, S.C., McKinley, J.P. and Resch, C.T. (1993) Cadmium sorption on specimen and soil smectites in sodium and calcium electrolytes. *Soil Science Society of America*, **57**, 1491–1501.

(*Received 11 August 2003; revised 8 December 2003; Ms. 827*)

https://doi.org/10.1346/CCMN.2004.0520307 Published online by Cambridge University Press